Medical Physics
The International Journal of Medical Physics Research and Practice

Investigating the accuracy of microstereotactic-body-radiotherapy utilizing anatomically accurate 3D printed rodent-morphic dosimeters

Steven T. Bache, Titania Juang, Matthew D. Belley, Bridget F. Koontz, John Adamovics, Terry T. Yoshizumi, David G. Kirsch, and Mark Oldham

Citation: Medical Physics **42**, 846 (2015); doi: 10.1118/1.4905489
View online: http://dx.doi.org/10.1118/1.4905489
View Table of Contents: http://scitation.aip.org/content/aapm/journal/medphys/42/2?ver=pdfcov
Published by the American Association of Physicists in Medicine

Investigating the accuracy of microstereotactic-body-radiotherapy utilizing anatomically accurate 3D printed rodent-morphic dosimeters

Steven T. Bache, Titania Juang, and Matthew D. Belley
Duke University Medical Physics Graduate Program, Durham, North Carolina 27705

Bridget F. Koontz
Duke University Medical Center, Durham, North Carolina 27710

John Adamovics
Rider University, Lawrenceville, New Jersey 08648

Terry T. Yoshizumi, David G. Kirsch, and Mark Oldham[a)]
Duke University Medical Center, Durham, North Carolina 27710

(Received 19 May 2014; revised 1 December 2014; accepted for publication 22 December 2014; published 22 January 2015)

Purpose: Sophisticated small animal irradiators, incorporating cone-beam-CT image-guidance, have recently been developed which enable exploration of the efficacy of advanced radiation treatments in the preclinical setting. Microstereotactic-body-radiation-therapy (microSBRT) is one technique of interest, utilizing field sizes in the range of 1–15 mm. Verification of the accuracy of microSBRT treatment delivery is challenging due to the lack of available methods to comprehensively measure dose distributions in representative phantoms with sufficiently high spatial resolution and in 3 dimensions (3D). This work introduces a potential solution in the form of anatomically accurate rodent-morphic 3D dosimeters compatible with ultrahigh resolution (0.3 mm^3) optical computed tomography (optical-CT) dose read-out.

Methods: Rodent-morphic dosimeters were produced by 3D-printing molds of rodent anatomy directly from contours defined on x-ray CT data sets of rats and mice, and using these molds to create tissue-equivalent radiochromic 3D dosimeters from Presage. Anatomically accurate spines were incorporated into some dosimeters, by first 3D printing the spine mold, then forming a high-Z bone equivalent spine insert. This spine insert was then set inside the tissue equivalent body mold. The high-Z spinal insert enabled representative cone-beam CT IGRT targeting. On irradiation, a linear radiochromic change in optical-density occurs in the dosimeter, which is proportional to absorbed dose, and was read out using optical-CT in high-resolution (0.5 mm isotropic voxels). Optical-CT data were converted to absolute dose in two ways: (i) using a calibration curve derived from other Presage dosimeters from the same batch, and (ii) by independent measurement of calibrated dose at a point using a novel detector comprised of a yttrium oxide based nanocrystalline scintillator, with a submillimeter active length. A microSBRT spinal treatment was delivered consisting of a 180° continuous arc at 225 kVp with a 20×10 mm field size. Dose response was evaluated using both the Presage/optical-CT 3D dosimetry system described above, and independent verification in select planes using EBT2 radiochromic film placed inside rodent-morphic dosimeters that had been sectioned in half.

Results: Rodent-morphic 3D dosimeters were successfully produced from Presage radiochromic material by utilizing 3D printed molds of rat CT contours. The dosimeters were found to be compatible with optical-CT dose readout in high-resolution 3D (0.5 mm isotropic voxels) with minimal artifacts or noise. Cone-beam CT image guidance was possible with these dosimeters due to sufficient contrast between high-Z spinal inserts and tissue equivalent Presage material (CNR ~10 on CBCT images). Dose at isocenter measured with optical-CT was found to agree with nanoscintillator measurement to within 2.8%. Maximum dose in line profiles taken through Presage and film dose slices agreed within 3%, with FWHM measurements through each profile found to agree within 2%.

Conclusions: This work demonstrates the feasibility of using 3D printing technology to make anatomically accurate Presage rodent-morphic dosimeters incorporating spinal-mimicking inserts. High quality optical-CT 3D dosimetry is feasible on these dosimeters, despite the irregular surfaces and implanted inserts. The ability to measure dose distributions in anatomically accurate phantoms represents a powerful useful additional verification tool for preclinical microSBRT. [http://dx.doi.org/10.1118/1.4905489]

Key words: 3D dosimetry, optical-CT, Presage, small animal irradiation, 3D printing

1. INTRODUCTION

In recent years, much effort has been given to the development of precise, image-guided small animal microirradiators for complex radiotherapy treatment in small animal tumor models.[1] Microirradiators enable exploration of the efficacy of novel radiation treatment approaches by providing the capability to reproduce realistic treatment delivery in small animal models.[2–7] Investigation of the efficacy and biological radio-response from new radiation treatments rely on the use of these small animal models before reaching the clinic. Preclinical studies aim to highlight the biological mechanisms governing radiotherapy response in many radiation applications.[8–11]

With more complex radiotherapy techniques being investigated comes a need for a high-resolution 3D measurement of dose distributions given by small animal microirradiators such as the X-Rad 225Cx (Precision X-Ray, N. Banford, CT). Current procedures for small animal treatment planning involve obtaining beam-on-time necessary for a prescribed dose from tabulated radiation output factors.[12] At present, there are no methods to comprehensively verify these delivery techniques due to the requirements for ultrahigh resolution and ability to measure the dose in 3 dimensions (3D). A high-resolution 3D dose readout is desired for radiotherapy treatments given by small animal irradiators, as well as for verification of treatment planning software, which is becoming more widely available.[13–16]

In this work, high-resolution rodent-morphic Presage radiochromic dosimeters (Heuris Inc., Skillman, NJ) were produced utilizing 3D printing technology in order to investigate the accuracy of end-to-end image-guided microstereotactic body radiation therapy (SBRT) arc treatment given by the X-Rad 225Cx microirradiator. We investigate (i) the feasibility of utilizing 3D printing in order to produce rodent-morphic Presage 3D dosimeters (including high-Z spinal inserts) directly from CT contours, (ii) the feasibility of optical-CT 3D dosimetry in these dosimeters exhibiting complex irregular shapes, and (iii) the application of (i) and (ii) to the verification of microSBRT treatments and comparison against independent dosimeters (EBT film and a novel scintillation point dose detector).

2. MATERIALS AND METHODS

Rodent-morphic dosimeters were manufactured from Presage, a polyurethane matrix doped with a radiochromic leuco-dye. The radiochromic response of Presage has been well documented and shown to exhibit a linear optical density change with respect to absorbed dose that is energy and dose-rate independent.[17–20] Presage dosimeters have been used in prior work to commission the X-Rad 225Cx small animal irradiator at Duke University and to verify the accuracy of cone beam CT image guidance.[12,21] The present work builds on this foundation by extension to the dosimetric validation of microSBRT treatments on rodent-morphic dosimeters. Evaluation of the rodent-morphic dosimeters involved (i) establishing the feasibility of manufacture both with and without high-Z heterogeneous inserts (such as bone), including verification of sufficient bony/soft-tissue contrast for representative CBCT IGRT positioning, (ii) achievability of dose-readout by optical-CT in high resolution (0.5 mm isotropic voxels), and (iii) absolute dose verification.

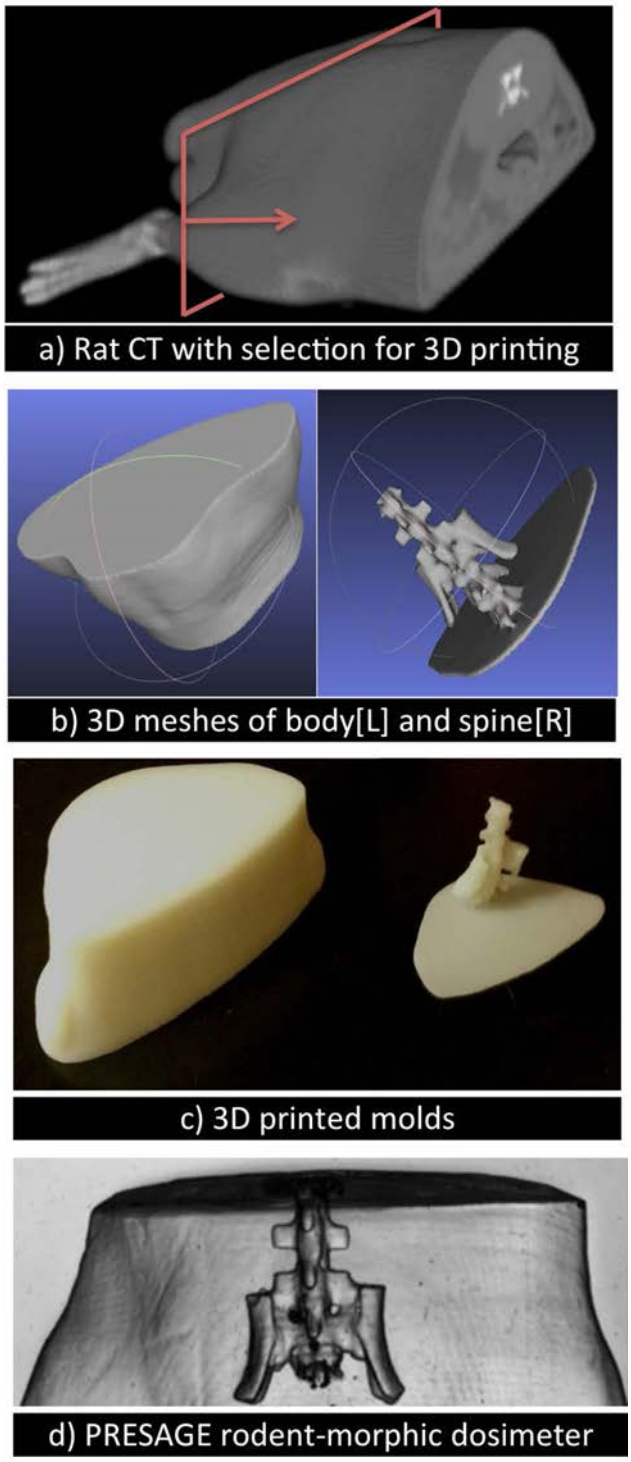

FIG. 1. Illustration of workflow for producing rodent-morphic dosimeters from CT data. Rodent CT data (a) are converted to 3D meshes (b) for printing 3D positive molds (c), which are used to make negative molds for constructing Presage dosimeters [(d)—optical-CT projection shown to highlight spinal insert].

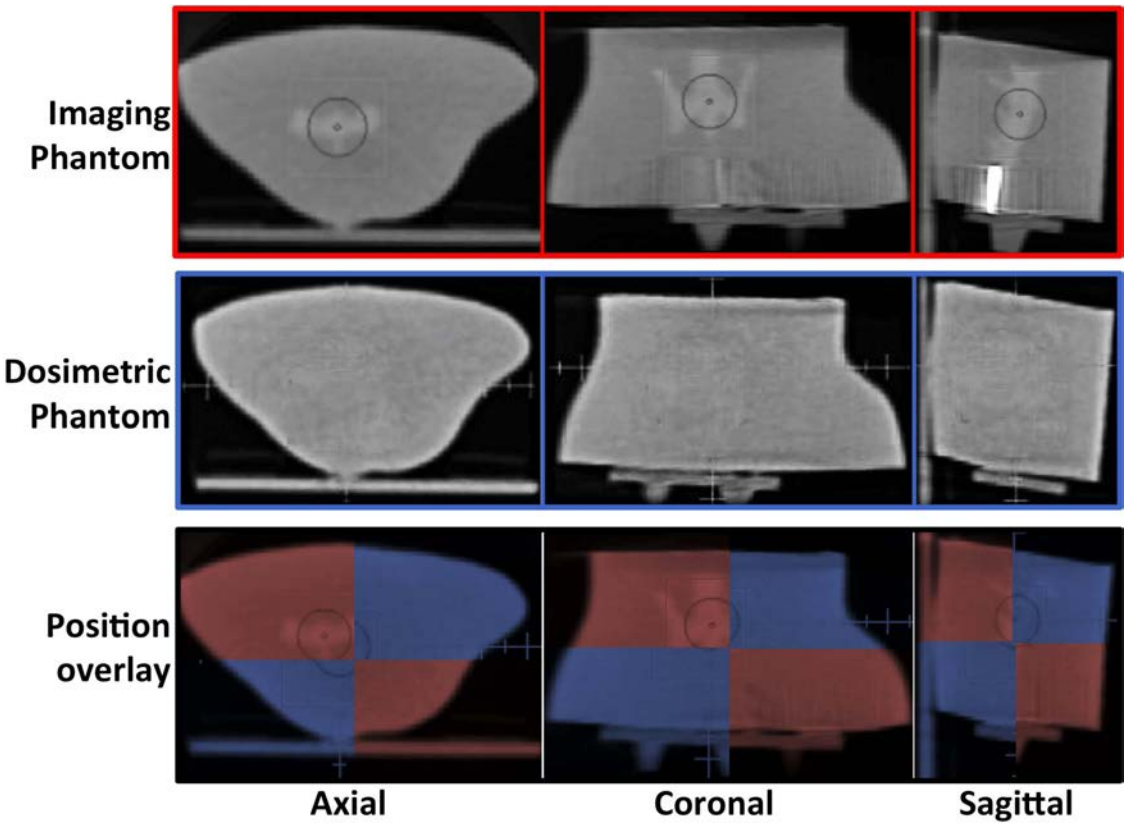

FIG. 2. CBCT of imaging (top row) and dosimetric (middle row) phantoms in three orthogonal views. Proper alignment can be seen in all three views with phantom images overlaid (bottom row). The high-Z spinal insert is visible in the imaging phantom, allowing isocenter targeting. Some artifacts remain—Top right: the high attenuation (bright white) artifact is produced by a small piece of metal remaining in the dosimeter from production. Imaging and isocenter placement is unaffected. Bottom row: the rings in the center are misaligned due to the images being taken before isocenter adjustment.

The general workflow for producing rodent-morphic dosimeters involved conversion of rodent CT data to 3D-printable file format,[22] and 3D-printing of positive molds to be used for making Presage dosimeters with anatomically correct outer contours and proper placement of high-Z Presage bony inserts. The specifics of this workflow are detailed below.

2.A. 3D dosimetry in rodent-morphic dosimeters

For this study, a research rat was scanned in the prone position, following IACUC protocols with a LightSpeed RT (GE Healthcare, UK) CT system at Duke University Medical Center Clinic at 80 kVp and 75 mAs. Volumetric CT data were exported as 0.625 mm axial slices in DICOM (.dcm) format, and imported into 3D Slicer (www.Slicer.org), an open-source software package for visualization and image analysis.[23] The 3D Slicer software gives the ability to contour structures and convert and export in stereolithography (.stl) file format. For this study, a central 40.1 mm axial portion of the rat was selected, corresponding to the prostate region plus 25 and 5 mm margins in the superior and inferior directions, respectively [Fig. 1(a)]. Both external body and spinal contours were drawn in 3D Slicer and saved as individual structures, first with automated Hounsfield units segmentation, then refined manually. Finer details outside of the vertebral bodies were omitted. A base with thickness 1.875 mm (3 axial CT slices) corresponding to the outer contours of the rat was added to the spinal insert. This allowed precise placement of the spine within the rat body by aligning the spinal insert base with the outer body base.

After segmentation, 3D-mesh files for rat spinal and outer body contours were imported into the MeshLab (meshlab.sourceforge.net) software package, an open-source package for editing and processing 3D triangular meshes. Additional post processing was performed in MeshLab in order to repair and smoothen the 3D files, including three Laplacian smoothing iterations, and deletion of any isolated volumes smaller than 5% of the maximum mesh volume. Smoothing was done to simplify the 3D printing as well as dosimeter manufacturing steps, while isolated volume deletion ensures the absence of any structures too small to be produced in the slice-by-slice manner used by the 3D printer [Fig. 1(b)].

Smoothed and processed spine and body .stl files were sent to be 3D printed by Fineline Prototyping (Raleigh, NC) via additive manufacturing, the process of building a model slice-by-slice from the bottom up using thin layers of rapidly cooling liquid plastics. Anatomical molds were printed in 0.1 mm slices from liquid DSM Somos ProtoGen 18420, a plastic-like photopolymer,[24] with 0.23 mm resolution in each in-slice dimension [Fig. 1(c)]. These molds served as the positive molds used in the production of the Presage rodent-morphic dosimeters.

3D rodent-morphic dosimeters were produced from 3D-printed molds in a three-step process. First, a flexible,

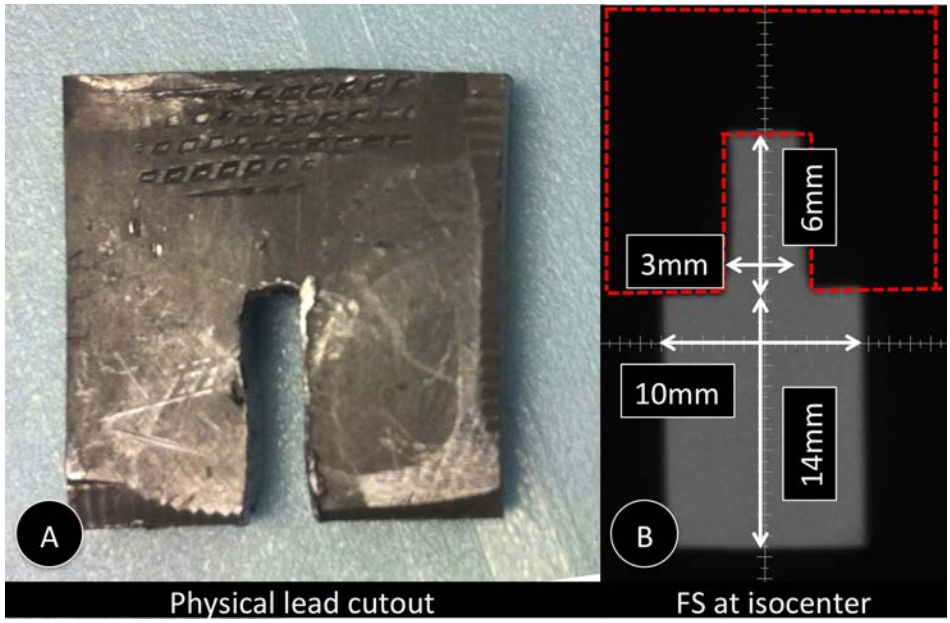

FIG. 3. (A) Lead block (~3 mm thick) cutout used to shape the radiation field into 10 and 3 mm width regions. (B) Radiographic projection image of the field at isocenter (dashed red lines indicate approximate block location).

removable mold was constructed from the 3D printed spinal mold. High-Z Presage material (Z_{eff} = 12.0, density 1.3 g/cm^3) was poured into the mold and cured (after several days) to produce a high attenuation spinal insert attached to a base matching the contours of the rat body. The spinal base ensured proper alignment of the spine with respect to the outer body contours in the next step. A similar removable mold was then produced using the 3D printed body contour. The spinal insert was placed into this body mold, and lower-Z (tissue equivalent) Presage material was poured into the mold around the spinal insert and cured. A second homogeneous dosimeter consisting of tissue-equivalent Presage was produced using the same removable outer contour mold. This resulted in two Presage radiochromic dosimeters derived directly from rat CT data [Fig. 1(d)], one with high-Z spinal insert for bone targeting and one homogeneous tissue-equivalent phantom for 3D dose measurement.

2.A.1. Optical-CT 3D dosimetry readout

Optical density change was read out using the Duke Mid-Sized Optical-CT System (DMOS),[30] in-house optical-CT system, which is a scaled-down version of the Duke Large-Field Optical-CT System (DLOS) described in Thomas *et al.*[25] The DMOS field of view is limited to an 11×15 cm field of view. Rather than match the ~100 μm pixel resolution of the CCD array, which would require over 3000 projections (π times the ~1000 matrix size), the DMOS was used with 360 projections taken at 1° increments. This has been shown in previous work to be adequate for reconstruction with (0.5 mm)^3

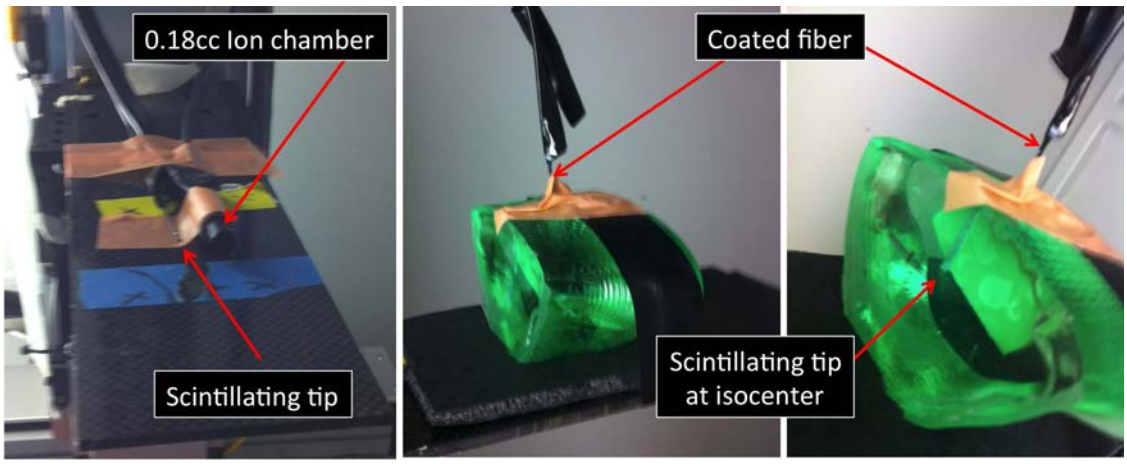

FIG. 4. Setup for absolute dose measurement at isocenter with a novel nanoscintillation detector. First, the detector was calibrated with a RadCal 0.18 cm^3 ion chamber (left), then, the 180° arc treatment was delivered three times with the scintillating detector placed at the rodent-morphic dosimeter isocenter (center, right).

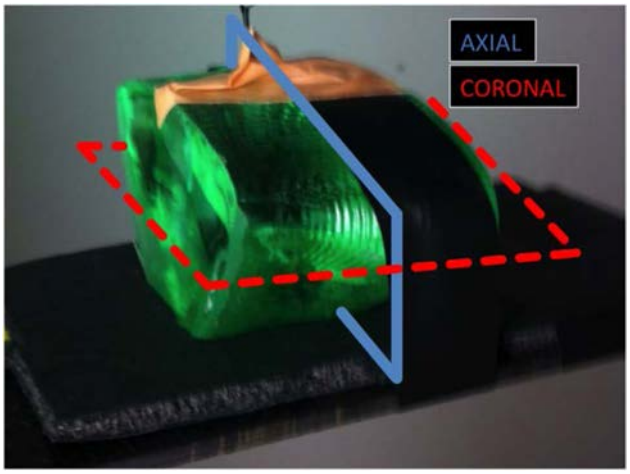

FIG. 5. Schematic showing placement of radiochromic film in axial (solid blue line) and coronal (dashed red line) planes for independent measurement of dose distributions.

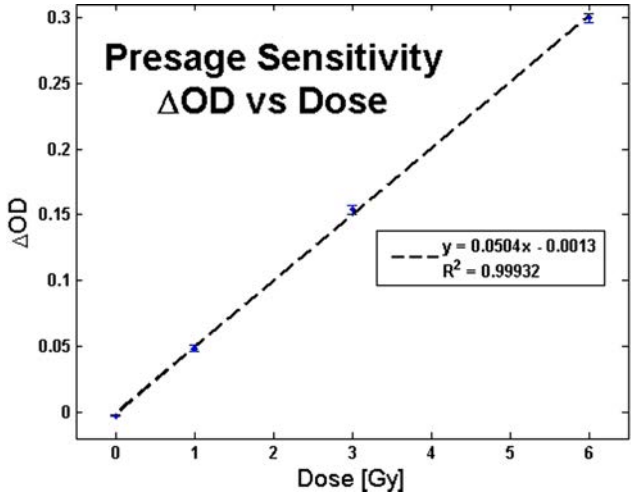

FIG. 7. Presage sensitivity in (ΔOD/Gy/cm) measured in small volume cuvette samples.

isotropic voxels.[19] Filtered back-projection reconstructions of optical density change were made with the iradon function as part of a custom MATLAB (MathWorks, Natick, MA). In order to calibrate the radiochromic sensitivity of the rodent-morphic Presage dosimeters, eight $1\times1\times4.5$ cm plastic volumes containing Presage material from the same batch used for rodent-morphic dosimeters were analyzed. Optical density at 633 nm was measured for each volume both pre- and post-irradiation with a Genesys 20 spectrophotometer (Thermo Spectronic, Waltham, MA). Irradiations were made at doses of 1, 3, and 6 Gy (two samples per dose and with two controls) with a 6 MV clinical beam. Sensitivity of the rodent-morphic dosimeters in ΔOD/Gy/cm was found from a linear fit of small volume sample data.

2.B. Treatment plan and delivery with CBCT-guided positioning

A treatment plan was devised in order to simulate SBRT spinal cord treatments given by a 180° arc. Accurate delivery to the rodent spine was accomplished using two rodent-morphic dosimeters: an "imaging" phantom that included the high-Z spinal insert for target alignment and isocenter placement, and a homogeneous "dosimetric" phantom for dose distribution readout. To achieve accurate spinal targeting, CBCT was performed on the imaging phantom and the isocenter was placed directly on the spine. The imaging phantom was then replaced on the carbon fiber treatment stage by the dosimetric phantom, preserving isocenter placement. Outer contour images were overlaid and compared in order to confirm exact replacement of the imaging phantom with the homogeneous dosimetric phantom (Fig. 2). A 2 cm (AP) × 1 cm rectangular cone was selected for treatment. A 3 mm lead-block (~4 HVLs at 225 kVp) was constructed and affixed to the treatment cone to divide the 2 cm longitudinal field into a 1 cm section and a 3 mm section at isocenter (Fig. 3). The field was divided to gain information on the concurrent rodent treatments being performed at Duke (1 cm beam width) and to test the ability of the dosimetric phantom to read out subcentimeter fields (3 mm width). The dosimeter was then treated in the supine position with a 180° arc at 225 kVp and 13 mAs through the treatment stage.

2.C. Independent verification with EBT film and nano-point-detector

To verify the accuracy of the Presage dose distribution, two measurements were made: a point-based dose measure-

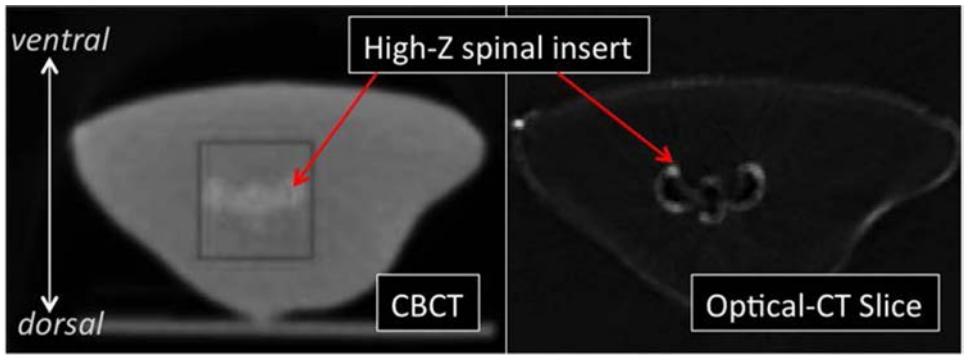

FIG. 6. Visibility of high-Z spinal insert in both CBCT (left) and Optical-CT (right) allows for accurate isocentric targeting.

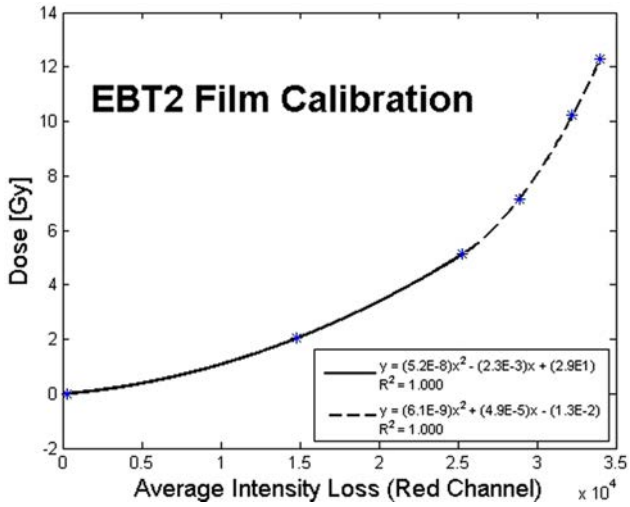

FIG. 8. Biquadratic fit of radiochromic film used for absolute dose verification.

ment at isocenter and a set of orthogonal 2D planar film measurements through the isocentric plane. For the point-dose measurement, first, a 1 mm channel was drilled into the original treated Presage dosimeter. NanoFOD (nano-fiber-optic detector), a novel europium and lithium doped yttrium oxide nanocrystal-based scintillation detector[26] was used to confirm dose at isocenter. The 600-μm active region of the detector was calibrated in units of integrated voltage (V s) vs exposure (mR) using a 0.18 cm^3 RadCal ion chamber through a series of nine 30-s open-field irradiations with the X-rad 225Cx irradiator—3 each at 8, 10, and 13 mAs. NanoFOD calibration factor was converted from V s/mR to soft-tissue dose in V s/cGy using the ICRU-44 formulation. The detector was then placed inside the Presage channel after setup on the X-Rad 225Cx treatment stage (Fig. 4). The original 180° arc treatment was repeated three times with the active region of the detector at treatment isocenter.

A second independent verification of dose was made with Gafchromic EBT2 radiochromic film (Ashland, Covington, KY). The radiochromic film was calibrated (in units of intensity loss/Gy) by irradiating several small pieces of film from the same film batch to known doses with a 6 MV treatment beam (energy dependence assumed negligible[27]), and comparing intensity (red channel counts) both pre- and post-irradiation through an Expression 10 000 XL flat bed film scanner (Epson America, Long Beach, CA). Average intensity loss for each film was measured and plotted vs dose and fitted with a high-dose and low-dose quadratic fit. In order

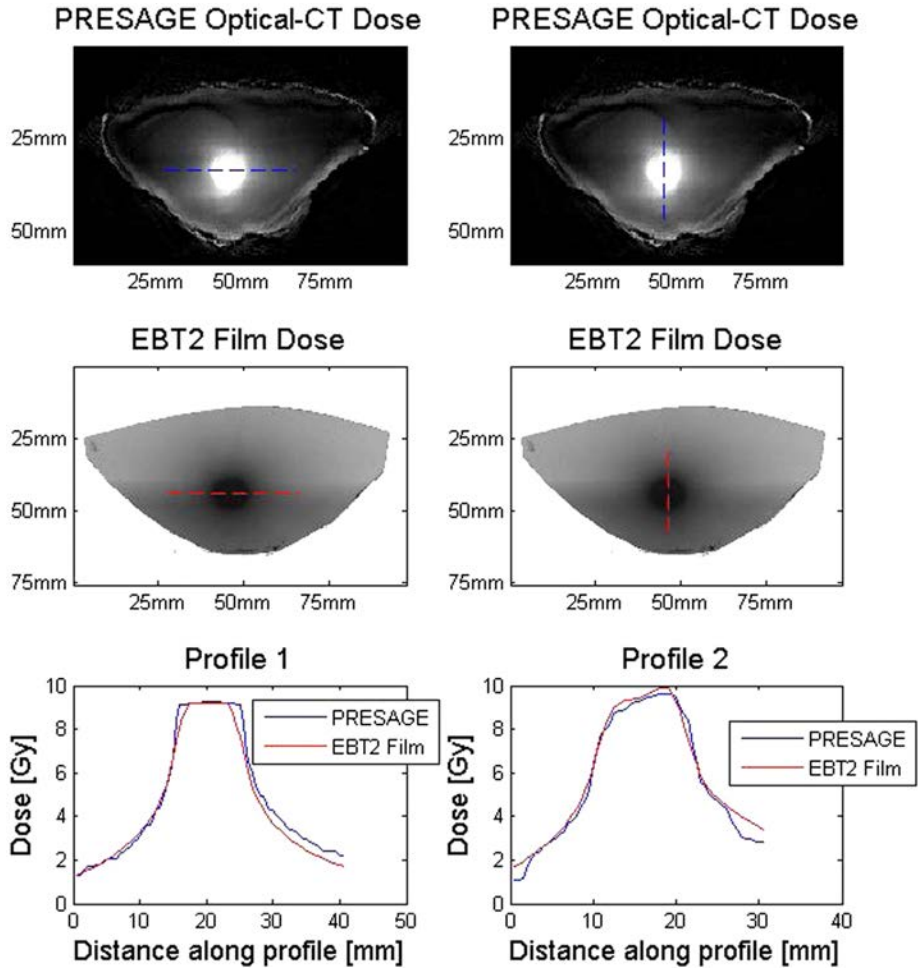

FIG. 9. Axial dose distributions measured with optical-CT (top row) and EBT2 film (middle row), with comparative line profiles (bottom row). Maximum dose/FWHM error was −2.6%/−0.7% for Profile 1 and −2.9%/−1.5% for Profile 2.

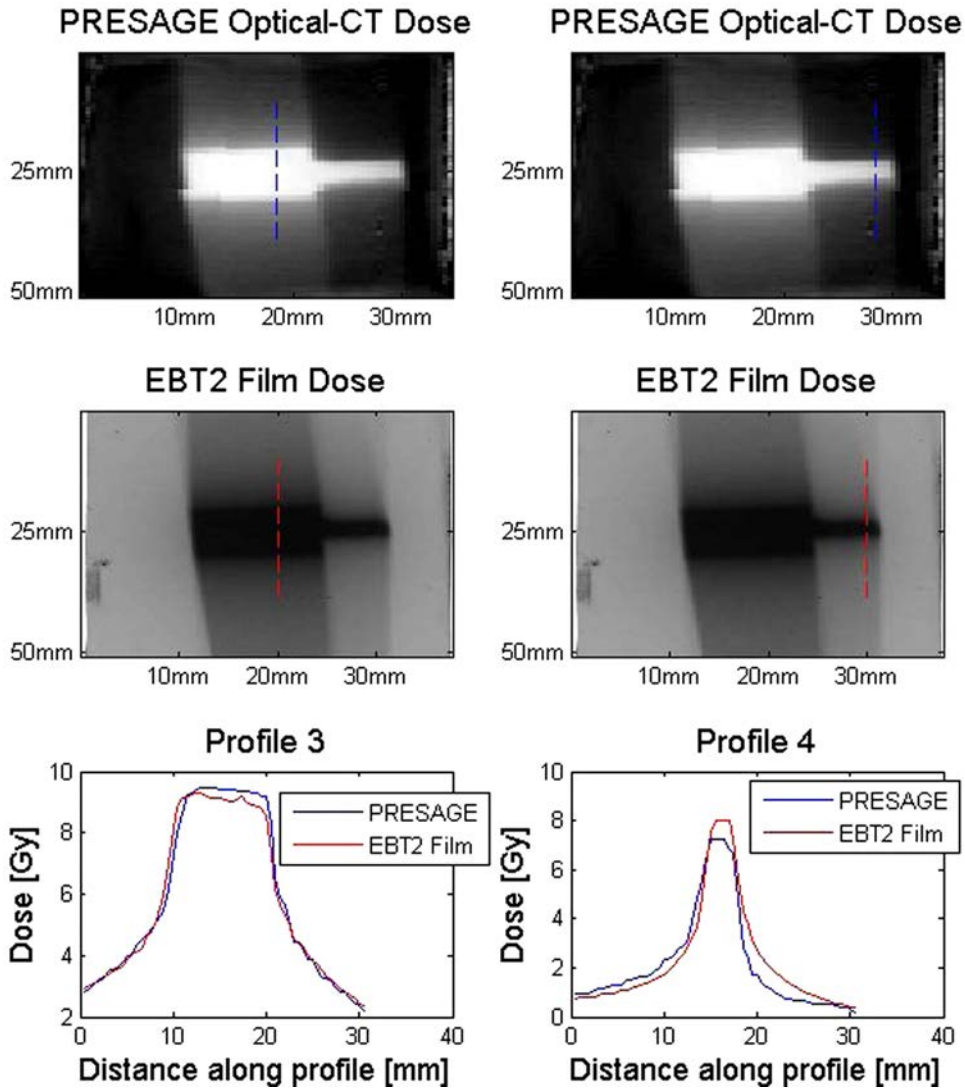

FIG. 10. Coronal dose distributions measured with optical-CT (top row) and EBT2 film (middle row), with comparative line profiles (bottom row). Maximum dose/FWHM error was 1.6%/−0.5% for Profile 3 and −6.7%/4.4% for Profile 4.

to verify dose distributions in two orthogonal planes, the two phantoms were machined in half along planes intersecting the isocenter, one along the coronal axis and one along the axial axis. Film was placed between the two halves and the 180° arc treatment was repeated for each dosimeter (Fig. 5). Intensity loss between pre- and post-irradiation scans of each film was converted to dose through the calibration fit equation.

3. RESULTS AND DISCUSSION

3.A. Production and image-guidance

Rodent-morphic dosimeters were produced with homogeneous tissue-equivalent Presage material with and without high-Z spinal inserts, directly from rat CT data. Because of the exact nature of 3D printing, dosimeters could be consistently produced. High Z spinal inserts were visible in X-Rad 225CX cone beam-CT and optical density reconstruction (Fig. 6), enabling accurate positioning and isocenter placement, as well as simplifying navigation about isocenter when analyzing dose. While the individual shapes of both the outer rat body and the spine were reproduced well, the relative positioning (i.e., the alignment of the spine within the body) was not exact (a millimeter or so discrepancy). This discrepancy arose because of a slight loss of alignment during curing of the Presage body dosimeter. This is not a fundamental limitation of the technique, rather an implementation aspect requiring further improvement.

3.B. Dose measurement with optical—CT

Figure 7 shows the sensitivity in ΔOD/cm of the rodent-morphic Presage vs dose in Gy. Presage sensitivity was found to exhibit a strong, linear radio-response ($R^2 = 0.99932$). Reconstructed voxel values in ΔOD were converted to dose through this linear relationship. Isocenter dose was determined within a ROI cube with a side length of 3 voxels (1.5 mm), centered about the arc isocenter. Mean isocenter dose was found to be 9.23 Gy with a 0.093 Gy standard deviation.

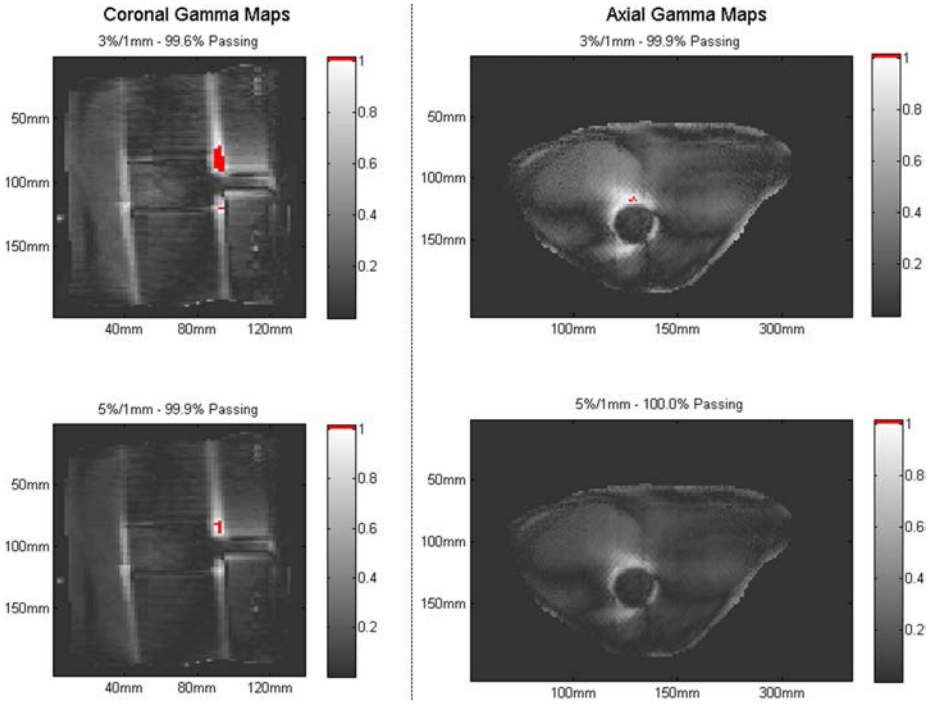

FIG. 11. Gamma maps comparing axial and coronal 2D Presage and film distributions at 1 mm distance-to-agreement 3% and 5% dose difference thresholds. Failing pixels accentuated for easy visualization.

3.C. Absolute dose verification

Absolute dose at isocenter was verified using the nanoFOD output calibration factor of 0.235 V s/cGy. The average converted tissue (and Presage) dose to isocenter for the three treatments with the nanoFOD inserted was found to be of 9.49 Gy (standard deviation = 0.0085 Gy), an absolute dose difference of 2.8% compared to optical density measurement of 9.23 Gy.

For planar film measurement verification, Fig. 8 shows the calibration equations used to convert film response to absolute dose.

Figures 9 and 10 show axial and coronal slices of Presage and film dose measurements, along with several line profiles through the isocentric dose region. Agreement between Presage and film was analyzed by computing difference in maximum dose and FWHM for each profile. Maximum dose difference calculated was below 3% and FWHM difference was below 2% between film and Presage for all profiles except for slight optical-CT dose under-estimation along the 3 mm narrow field. The narrow field maximum dose difference was 6.7%, with FWHM difference of 4.4%. Further investigation is required to reconcile this dose difference, which may be caused due to a stray light artifact that has been shown in previous work to affect regions of steep dose gradients with small fields.[28] To account for slight error in film/Presage registration, gamma maps were also calculated with 1 mm distance-to-agreement at the 3% and 5% dose difference thresholds (Fig. 11). Table I summarizes the agreement between Presage and film.

3.D. Clinical interpretation

One potential benefit of rodent-morphic dosimeters is the ability to overlay dose distributions directly onto original rodent CT data. Figure 12 shows microSBRT dose distributions in axial and coronal planes. Distributions as presented are assumed in homogeneous tissue. Future work is required for modification of dose from homogenous to heterogeneous rodent composition (along the lines shown in Oldham *et al.*[29]), including an investigation of optical-CT readout in Presage dosimeters with heterogeneous inserts (such as spinal imaging insert presented in this work).

TABLE I. Presage difference with respect to film in maximum dose and FWHM (line profiles) and 2-D gamma pass rates taken in two orthogonal planes at 1 mm distance-to-agreement and 3%/5% dose difference.

	Line profiles			Gamma pass rate	
Plane	Line	Max dose diff (%)	FWHM diff (%)	3% 1 mm	5% 1 mm
Axial	Left/right	−2.6	−0.7	99.9%	100.0%
	Ventral/dorsal	−2.9	−1.5		
Coronal	10 mm Field	1.6	−0.5	99.6%	99.9%
	3 mm Field	−6.7	4.4		

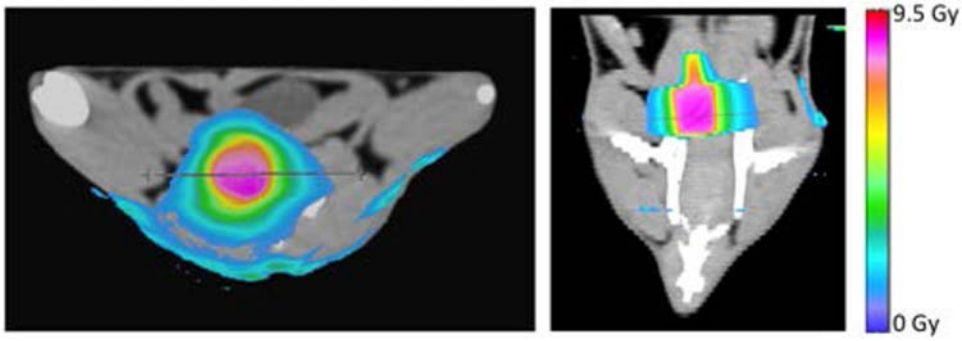

FIG. 12. 3D dose distributions overlaid on original rat CT used for 3D printing in axial (left) and coronal (right) planes. In this case, dose to homogeneous tissue-equivalent Presage was overlaid directly onto heterogeneous rodent data. Future work will involve dose distributions to heterogeneous rodent-morphic dosimeters.

4. CONCLUSION

This work demonstrates the feasibility of accurate 3D dosimetry in high-resolution rodent-morphic phantoms for small animal microirradiators. Variable density Presage provided adequate contrast to be a viable method of CBCT targeting and isocenter placement on the X-Rad 225Cx irradiator, while optical-CT readout provides an accurate dose measurement when compared to direct exposure measurement. While this study focused on rat spine and outer body contours, any contour of interest may be segmented, converted to a 3D-printable file, and made into a mold for anatomically accurate Presage phantoms. This method of dose measurement allows for high-resolution of complex treatment paradigms being used in the preclinical setting and enhances the robustness of tumor biology and radio-response studies in the small animal regime.

ACKNOWLEDGMENTS

The authors would like to thank Hooney Min for help with irradiations and Ron Benning for help with dosimeter production. This work was supported, in part, by NIH R01CA100835, as well as grants from the U. S. NRC Health Physics Fellowship Grant (No. NRC-HQ-12-G-38-0022), and the National Institute of Allergy and Infectious Diseases (5U19AI067798).

[a]Author to whom correspondence should be addressed. Electronic mail: mark.oldham@duke.edu

[1]F. Verhaegen, P. Granton, and E. Tryggestad, "Small animal radiotherapy research platforms," Phys. Med. Biol. **56**, R55–R83 (2011).
[2]M. Matinfar, I. Iordachita, E. Ford, J. Wong, and P. Kazanzides, "Precision radiotherapy for small animal research," Med. Image Comput. Comput. Assist. Interv. Int. Conf. Med. Image Comput. Comput. Assist. Interv. **11**, 619–626 (2008).
[3]M. Rodriguez and R. Jeraj, "Design of a radiation facility for very small specimens used in radiobiology studies," Phys. Med. Biol. **53**, 2953–2970 (2008).
[4]J. Wong, E. Armour, P. Kazanzides, I. Iordachita, E. Tryggestad, H. Deng, M. Matinfar, C. Kennedy, Z. Liu, T. Chan, O. Gray, F. Verhaegen, T. McNutt, E. Ford, and T. L. Deweese, "High-resolution, small animal radiation research platform with x-ray tomographic guidance capabilities," Int. J. Radiat. Oncol., Biol., Phys. **71**, 1591–1599 (2008).
[5]M. Matinfar, I. Iordachita, J. Wong, and P. Kazanzides, "Robotic delivery of complex radiation volumes for small animal research," in *IEEE International Conference on Robotics and Automation: ICRA* (IEEE, Anchorage, AK, 2010), pp. 2056–2061.
[6]K. H. Song, R. Pidikiti, S. Stojadinovic, M. Speiser, S. Seliounine, D. Saha, and T. D. Solberg, "An x-ray image guidance system for small animal stereotactic irradiation," Phys. Med. Biol. **55**, 7345–7362 (2010).
[7]P. E. Lindsay, P. V. Granton, A. Gasparini, S. Jelveh, R. Clarkson, S. van Hoof, J. Hermans, J. Kaas, F. Wittkamper, J. J. Sonke, F. Verhaegen, and D. A. Jaffray, "Multi-institutional dosimetric and geometric commissioning of image-guided small animal irradiators," Med. Phys. **41**, 031714 (12pp.) (2014).
[8]R. Clarkson, P. E. Lindsay, S. Ansell, G. Wilson, S. Jelveh, R. P. Hill, and D. A. Jaffray, "Characterization of image quality and image-guidance performance of a preclinical microirradiator," Med. Phys. **38**, 845–856 (2011).
[9]M. Dewhirst, G. Palmer, A. Fontanella, and M. Boss, "Biological considerations for failure to acheive full thermal ablation," presented at the STM Spring Conference, Washington, DC (2013) (unpublished).
[10]A. Maeda, M. K. Leung, L. Conroy, Y. Chen, J. Bu, P. E. Lindsay, S. Mintzberg, C. Virtanen, J. Tsao, N. A. Winegarden, Y. Wang, L. Morikawa, I. A. Vitkin, D. A. Jaffray, R. P. Hill, and R. S. DaCosta, "*In vivo* optical imaging of tumor and microvascular response to ionizing radiation," PLoS One **7**, e42133 (2012).
[11]M. Matinfar, O. Gray, I. Iordachita, C. Kennedy, E. Ford, J. Wong, R. H. Taylor, and P. Kazanzides, "Small animal radiation research platform: Imaging, mechanics, control and calibration," Med. Image Comput. Comput. Assist. Interv. Int. Conf. Med. Image Comput. Comput. Assist. Interv. **10**, 926–934 (2007).
[12]J. Newton, M. Oldham, A. Thomas, Y. Li, J. Adamovics, D. G. Kirsch, and S. Das, "Commissioning a small-field biological irradiator using point, 2D, and 3D dosimetry techniques," Med. Phys. **38**, 6754–6762 (2011).
[13]R. Pidikiti, S. Stojadinovic, M. Speiser, K. H. Song, F. Hager, D. Saha, and T. D. Solberg, "Dosimetric characterization of an image-guided stereotactic small animal irradiator," Phys. Med. Biol. **56**, 2585–2599 (2011).
[14]P. V. Granton and F. Verhaegen, "On the use of an analytic source model for dose calculations in precision image-guided small animal radiotherapy," Phys. Med. Biol. **58**, 3377–3395 (2013).
[15]S. J. van Hoof, P. V. Granton, and F. Verhaegen, "Development and validation of a treatment planning system for small animal radiotherapy: SmART-Plan," Radiother. Oncol. **109**, 361–366 (2013).
[16]F. Verhaegen, S. van Hoof, P. V. Granton, and D. Trani, "A review of treatment planning for precision image-guided photon beam pre-clinical animal radiation studies," Z. Med. Phys. **24**, 323–334 (2014).
[17]M. Maryanski and J. Adamovics, "OCT scanning properties of PRESAGE -A 3D radiochromic solid polymer dosimeter," Med. Phys. **31**(6), 1906 (2004).
[18]J. Adamovics and M. J. Maryanski, "Characterisation of PRESAGE: A new 3-D radiochromic solid polymer dosemeter for ionising radiation," Radiat. Prot. Dosim. **120**, 107–112 (2006).

[19]H. S. Sakhalkar and M. Oldham, "Fast, high-resolution 3D dosimetry utilizing a novel optical-CT scanner incorporating tertiary telecentric collimation," Med. Phys. **35**, 101–111 (2008).
[20]T. Gorjiara, R. Hill, Z. Kuncic, J. Adamovics, S. Bosi, J. H. Kim, and C. Baldock, "Investigation of radiological properties and water equivalency of PRESAGE dosimeters," Med. Phys. **38**, 2265–2274 (2011).
[21]L. J. Rankine, J. Newton, S. T. Bache, S. Das, J. Adamovics, D. G. Kirsch, and M. Oldham, "Investigating end-to-end accuracy of image guided radiation treatment delivery using a micro-irradiator," Phys. Med. Biol. **58**, 7791–7801 (2013).
[22]E. Doney, L. A. Krumdick, J. M. Diener, C. A. Wathen, S. E. Chapman, B. Stamile, J. E. Scott, M. J. Ravosa, T. Van Avermaete, and W. M. Leevy, "3D printing of preclinical x-ray computed tomographic data sets," J. Visualized Exp. **73**, e50250 (2013).
[23]A. Fedorov, R. Beichel, J. Kalpathy-Cramer, J. Finet, J. C. Fillion-Robin, S. Pujol, C. Bauer, D. Jennings, F. Fennessy, M. Sonka, J. Buatti, S. R. Aylward, J. V. Miller, S. Pieper, and R. Kikinis, "3D slicer as an image computing platform for the quantitative imaging network," Magn. Reson. Imaging **30**, 1323–1341 (2012).
[24]See www.dsmsomos.com for "Somos Protogen 18420 material data Safety Sheet" (accessed 2013).
[25]A. Thomas, J. Newton, J. Adamovics, and M. Oldham, "Commissioning and benchmarking a 3D dosimetry system for clinical use," Med. Phys. **38**, 4846–4857 (2011).
[26]I. Stanton, M. Belley, G. Nguyen, A. Rodrigues, Y. Li, D. Kirsch, T. Yoshizumi, and M. Therien, "Europium- and lithium-doped yttrium oxide nanocrystals that provide a linear emissive response with x-ray radiation exposure," Nanoscale **6**(10), 5284–5288 (2014).
[27]B. Arjomandy, R. Tailor, A. Anand, N. Sahoo, M. Gillin, K. Prado, and M. Vicic, "Energy dependence and dose response of Gafchromic EBT2 film over a wide range of photon, electron, and proton beam energies," Med. Phys. **37**(5), 1942–1947 (2010).
[28]A. Thomas, M. Pierquet, K. Jordan, and M. Oldham, "A method to correct for spectral artifacts in optical-CT dosimetry," Phys. Med. Biol. **56**, 3403–3416 (2011).
[29]M. Oldham, A. Thomas, J. O'Daniel, T. Juang, G. Ibbot, J. Adamovics, and J. Kirkpatrick, "A quality assurance method that utilizes 3D dosimetry and facilitates clinical interpretation," Int. J. Radiat. Oncol., Biol., Phys. **84**(2), 540–546 (2012).
[30]T. Juang, R. Grant, J. Adamovics, G. Ibbott, and M. Oldham, "On the feasibility of comprehensive high-resolution 3D remote dosimetry," Med. Phys. **41**, 071706 (11pp.) (2014).